

# Metal Complexes of Curcumin: A Comprehensive Approach to Design, Synthesis, Characterization and Assessment of Anti-tubercular Activity

Paramita Das<sup>1,\*</sup>, Yamuna HM<sup>1</sup>, Harshashree M<sup>1</sup>, Raman Dang<sup>2</sup>

<sup>1</sup>Department of Pharmaceutical Chemistry, Krupanidhi College of Pharmacy, Chikkabellanduru, Carmelaram Post, Varthur, Bangalore, Karnataka, INDIA.

<sup>2</sup>Principal, Krupanidhi College of Pharmacy, Bangalore, Karnataka, INDIA.

## ABSTRACT

**Background:** The primary challenge facing Tuberculosis (TB) is the growing prevalence of drug resistance and the hepatotoxicity secondary effects of first and second-line anti-TB treatments have reignited interest in exploring new metal drug complexes as possible sources of anti-TB medications. **Aim:** To perform *in silico* studies for Curcumin-metal complexes, synthesis and evaluate their antitubercular activity and cytotoxicity. **Materials and Methods:** Designed metal complexes were docked against 2NSD and performed ADMET studies. Based on binding affinity, a series of Curcumin-metal complexes were synthesized, characterized by IR, NMR, MASS, P-XRD and the antitubercular activity was evaluated by MABA and MTT assay for cytotoxicity investigations. **Results and Discussion:** The binding energies ranged from -8.0 to -10.1 'kcal/mol'. At -10.1 'kcal/mol', the Curcumin-Cu complex (C1) exhibited the best binding. The synthesized compounds were evaluated against *Mycobacterium tuberculosis* (H37Rv) using the MABA assay. Curcumin-Cu complex (C1) showed the highest activity and was the most sensitive at 0.8 µg/mL and showed less toxicity with an IC<sub>50</sub> of 10.0 and a selectivity index of 4.0. Cytotoxicity was evaluated by the ATCC CCL-81 cell line. **Conclusion:** Therefore, we can conclude that the molecular hit will be a good lead to develop novel therapies for tuberculosis treatment.

**Keywords:** Tuberculosis, Curcumin metal complex, Docking, ADMET studies, MABA assay.

## Correspondence:

**Dr. Paramita Das**

Department of Pharmaceutical Chemistry, Krupanidhi College of Pharmacy, #12/1 Chikkabellanduru, Carmelaram Post, Varthur, Bangalore-560035, Karnataka, INDIA.  
Email: paramitadas04@gmail.com

**Received:** 07-02-2024;

**Revised:** 15-03-2024;

**Accepted:** 20-04-2024.

## INTRODUCTION

The greatest barrier to tuberculosis chemotherapy is the rise in drug resistance to approved therapeutic treatments. The causative agent of tuberculosis is *Mycobacterium tuberculosis*, which is a major worldwide health emergency with millions of deaths recorded in a year.<sup>1</sup> The primary categories of antitubercular drugs mainly target processes such as cell wall production, mycolic acids, Arabinogalactan and DNA replication within bacterial cells. Unfortunately, each of these mechanisms is vulnerable to the development of bacterial resistance.<sup>2</sup> Multidrug-Resistant Tuberculosis (MDR-TB) is characterized by resistance to at least isoniazid and rifampicin, while Extensively Drug-Resistant Tuberculosis (XDR-TB) goes a step further by exhibiting resistance to second-line injectable drugs and fluoroquinolones. This necessitates long-term therapies, exposing patients to a higher risk of adverse effects.<sup>3</sup> One of the most

common side effects of anti-TB treatment is drug-induced liver damage (hepatotoxicity).<sup>4</sup> Similarly, the growing demand for novel treatments is exacerbated by the dwindling effectiveness of already available anti-TB medications and the emergence of resistant strains. This called for more research into discovering novel chemical entities with distinctive modes of action, especially in light of a rise in drug resistance. Curcumin-based transition metal complexes are gaining interest lately as potential antitubercular medications. In order to overcome resistance and increase activity, metal coordination to physiologically active molecules is helpful.<sup>5,6</sup> Numerous studies have shown that Curcumin and metal ions coordinate to enhance the anticancer,<sup>7</sup> antioxidant,<sup>8</sup> and antibacterial effects.<sup>9</sup> A review of the literature reveals that while metals act as cytotoxic stimulators for the ligands, the ligand molecules are less active than their transition metal complexes.<sup>10</sup>

Curcumin possesses antitubercular effect and a wide spectrum of pharmacological characteristics research into its potential use as a chemotherapeutic is still going on.<sup>11</sup> In recent decades, curcumin complexes with different metal salts have been synthesised to overcome curcumin's limitations and increase its physiological activity. The overall structure of curcumin is altered



DOI: 10.5530/ijper.58.3s.96

### Copyright Information :

Copyright Author (s) 2024 Distributed under Creative Commons CC-BY 4.0

Publishing Partner : EManuscript Tech. [www.emanuscript.in]

and its biological activity is increased when metals interact with ligand. Carbonyl group stability at the diketone moiety has been affected by the metal ion coordination. Metals can act as enzyme coactivators and Curcumin-metal complexes can interact with enzyme active sites to stimulate a variety of biological functions.<sup>12</sup> Pharmacological studies have demonstrated that Curcumin-metal complexes have a potent anti-TB action.<sup>13</sup>

Taking along every aspect that was previously discussed, this study presents the synthesis of curcumin in addition to its metal complexes using metal salts. Each compound was investigated using various spectroscopic and analytical techniques. The synthesised compounds were examined for their *in vitro* antimycobacterial activity and cytotoxicity profiles using the MABA and MTT assays.

## MATERIALS AND METHODS

The synthetic grade was used for the chemicals and solvents. Curcumin and metal salts were acquired from Sigma Aldrich, whereas ethanol, dichloromethane and chloroform were acquired from CSC Fine Chemicals and purified in accordance with industry standards.

An electrothermal instrument employing capillary tubes were used to calculate the melting point and is uncorrected. The FT-IR graph of the compounds were obtained by Bruker (Alpha 2) FT-IR Spectrophotometer in the range of 4000-400  $\text{cm}^{-1}$ . By using a Bruker Avance Neo (500 MHz) instrument in DMSO as the solvent and TMS as the internal reference chemical the  $^1\text{H}$  NMR spectra was obtained. The Electrospray Ionization technique (ESI-MS) was utilized to capture the spectra of all substances. This was achieved by employing a WATERS-XEVO G2-XS-QToF mass spectrometer. For the compounds under investigation, the X-ray powder diffraction profiles were produced. This process involved the utilization of a Bruker D8 Advance model Powder X-ray Diffractometer, spanning a diffraction angle range of  $10^\circ$  to  $90^\circ$ , where the Bragg angle is denoted as  $\theta$ .

### Molecular Docking Studies

Using a conventional procedure, a protein (PDB ID: 2NSD) and developed compounds were docked at their active site. The chemical structures of the ligands was drawn by Chem Draw 18.0 with appropriate 2D directions and the energy of all molecule were decreased by using ChemBio3D. According to literature, the co-crystallized ligand,  $\text{H}_2\text{O}$  molecules and cofactors were removed to generate the protein Enoyl Co-A reductase (PDB ID: 2NSD) structure.<sup>14</sup> The appropriate residues were kept with the protein file when the target protein was produced. The docking grid box was constructed using a graphical user interface. The grid box has a 0.667 grid point spacing and consists of 44, 47 and 29 points in the x, y and z dimensions, respectively. The grid box observed at 62Å, 62Å and 69Å. Pymol (2.5.3) was used to visually

assess the results and Discovery Studios was used to observe the 2D interactions.<sup>15</sup>

### *In silico* drug-likeness properties of the compounds

Lipinski had previously proposed that molecules have drug-like properties. Initially, all synthesised chemical structures were drawn in ChemDraw 18.0 to collect isomeric SMILES (Simplified Molecular-input Line-entry System) in SD file format. The *in silico* pharmacokinetics of isolated compounds were calculated using the Swiss ADME approach, which included the number of rotatable bonds, hydrogen bond donors, hydrogen bond acceptors and TPSA (Topological Polar Surface Area).<sup>16</sup> Osiris Property Explorer were used to calculate on-the-fly several drug-relevant properties and also used to forecast physicochemical and toxicological features, which must be optimised while creating pharmaceutically active molecules.<sup>17</sup>

### Synthesis of Curcumin-metal complexes

Metals were used as the core atom for the formation of Curcumin-metal complexes. The numerous metal salts were combined with the curcumin in a 1:2 ratio. The complex were developed by combining pure curcumin with metal salts in an ethanol solution at a ratio of 1:2. Curcumin (3 g, 8.16 mmol) was dissolved in 50 mL of pure ethanol and heated to  $60^\circ\text{C}$  in an atmospheric nitrogen. Metal salts were dissolved in 100 mL of ethanol and heated to dissolve. The ethanolic solution of metal salts was immediately added to ethanolic solution of Curcumin and the coloured precipitate was generated. The mixture was refluxed in atmospheric nitrogen for 4 hr at  $40^\circ\text{C}$ . In order to procure the complex, the solid result was filtered and rinsed with cold ethanol and water to remove any remaining reactants before drying.

### Anti-tuberculosis activity

The synthesised compounds were evaluated for *Mycobacterium tuberculosis* (H37Rv) using Microplate Alamar Blue Assay (MABA). The wells were incubated at  $37^\circ\text{C}$  for 5 days with dosages ranging from 100 to 0.8  $\mu\text{g}/\text{mL}$  followed with an Alamar Blue reagent and 10% Tween 80 solution for 24hrs. The absence of bacterial growth was shown by the colour blue and the presence of bacterial growth was indicated by the colour pink. The Minimum Inhibitory Concentration (MIC) is the minimum drug concentration required to prevent the colour change from blue to pink and all the compounds were evaluated against standard drugs like rifampicin, isoniazid and ethambutol.<sup>18</sup>

### Cytotoxicity studies

*In vitro* cytotoxicity on *M. tuberculosis* cell lines, specifically Vero cells ATCC CCL-81 were investigated for several dosages of synthesised compounds. It relies on the theory that MTT (3-(4,5-dimethylthiazol-2-yl)-2,5-diphenyltetrazolium bromide) is absorbed by active cells and metabolised into a blue formazan

product. Briefly stated, relevant controls were placed in triplicate wells of 96-well culture plates containing tuberculous cells and the cells were cultivated at 37°C in a CO<sub>2</sub> incubator. The experiment was carried out for 72 hr after adding MTT solution of 25 mL (5 mg/mL) to each. The Prism software version 4.01 was used to calculate the IC<sub>50</sub> values using a nonlinear regression model.<sup>19</sup>

## RESULTS AND DISCUSSION

### Docking studies

For the assessment of binding energies required to create complex and molecular interactions, a computational approach was employed. The ten compounds were subjected to design and optimization within the active binding site of Enoyl-CoA reductase. Among these compounds, namely C1, C3 and C7, demonstrated the most favourable binding energies, measuring at -10.1, -9.8 and -9.0 Kcal/mol, respectively. Notably, C1 exhibited the most favourable binding energy with the Enoyl CoA reductase (Figure 1) domain at -10.1 Kcal/mol. This binding was facilitated by the formation of hydrogen bonds with ASP148 and ILE15, as well as  $\pi$ - $\pi$  interactions with PHE149, as depicted in (Figure 2) and docked view were given in (Figure 3) A comprehensive summary of the docking results can be found in (Table 1).

The outcomes of the *in silico* ADMET properties were presented in (Table 2). When compared to the ligand, the synthesised metal complexes had the highest TPSA (154.76 Å). None of the ligand molecules and synthesised compounds exhibit any mutagenicity, tumorigenicity, reproductive toxicity, or eye irritation.

### Synthesis

Based upon the docking results the 10 curcumin complexes were synthesized and were found to be colourless solids at room temperature. The synthesised compounds were found to have a melting point of more than 300°C and are soluble in organic solvents such as DMSO, DMF, ethanol and chloroform (Table 3).

### FTIR

The FT-IR spectra of Curcumin ligand and synthesised metal complexes were collected in the 4000-400 cm<sup>-1</sup> region. The experimental outcomes are displayed in Table 4. When compared to the Curcumin spectra, the Curcumin-metal complex spectrum displays differences in the vibrational absorption wavenumbers, peak strength and peak shape. The metal complexes were shifted to a lower frequency area band at 3336 cm<sup>-1</sup> of phenolic -OH due to intra and inter molecule hydrogen bonding. The C=O enol stretching vibration absorption band also changes, the free ligand exhibiting a sharp and strong absorption peak at 1626 cm<sup>-1</sup>, whereas the Curcumin-metal complex exhibits no peak or may be

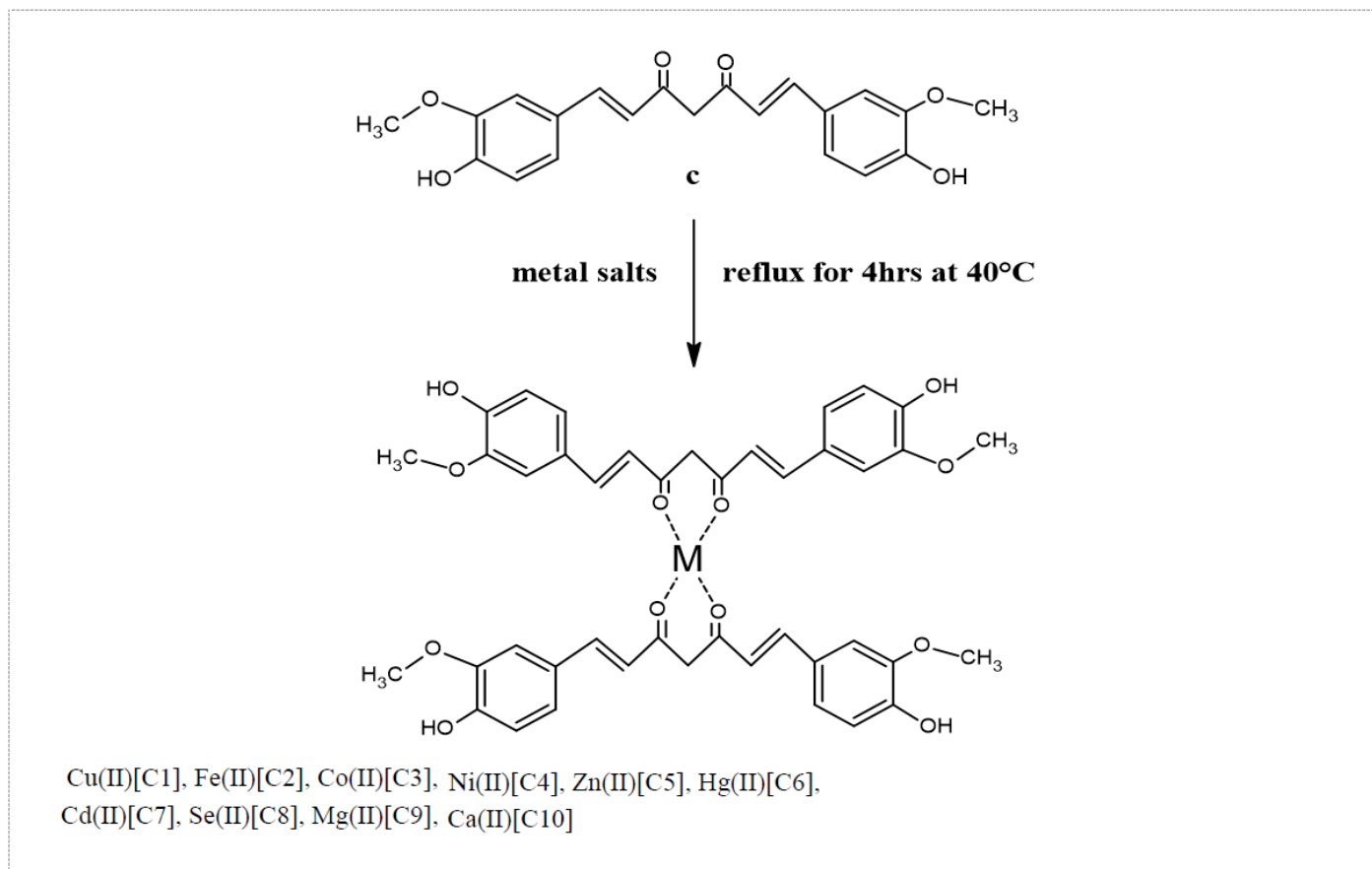
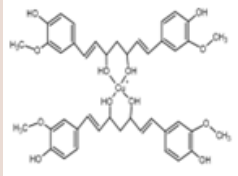
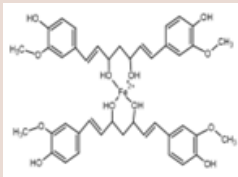
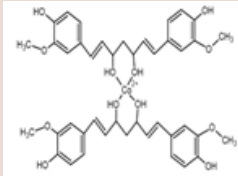
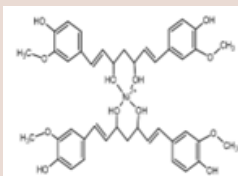
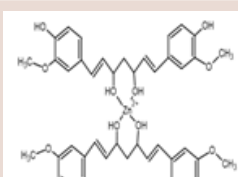
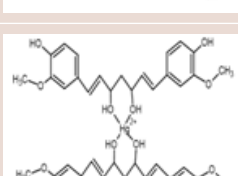
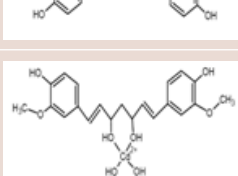
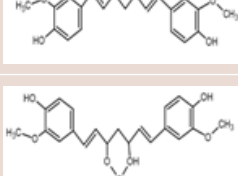
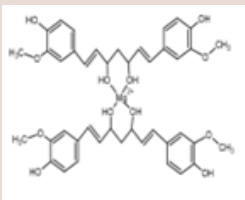
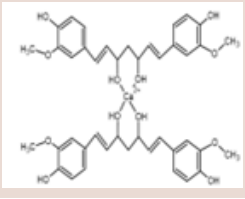


Figure 1: Scheme -Synthesis of Curcumin metal complexes.

**Table 1: Docking outcomes for Enoyl CoA-targeting Compounds (PDB ID: 2NSD).**

Sl. No.	Structure	Compound	Target	Binding Energy ('kcal/mol')	H-bonding	Interactions
1		C1	ECH_2NSD	-10.1	2H	ASP148,ILE15,PHE149
2		C2	ECH_2NSD	-8.9	1H	ASN231,LEU250,ALA244,LYS240,ILE228,HIS265
3		C3	ECH_2NSD	-9.8	3H	GLY14,SER94,GLN100,ALA203,TYR199
4		C4	ECH_2NSD	-8.3	2H	ASP141,VAL189,GLY14,PHE17
5		C5	ECH_2NSD	-8.3	1H	SER94,PHE41,PRO99,ALA206,ILE122,ILE95,ALA198
6		C6	ECH_2NSD	-8.8	0	TYR125,HIS121,SER170
7		C7	ECH_2NSD	-9.0	0	PHE41,MET98,ILE202,THR99
8		C8	ECH_2NSD	-8.8	4H	ASP42,TYR158,VAL65,LEU63,PHE41

Sl. No.	Structure	Compound	Target	Binding Energy ('kcal/mol')	H-bonding	Interactions
9		C9	ECH_2NSD	-8.8	1H	ASP150,PRO151,SER152,ARG153,ALA154
10		C10	ECH_2NSD	-8.0	0	SER152,ARG153,ALA154,MET155,PRO156

**Table 2: In silico drug likeness properties and Toxicity results of Curcumin and its metal complexes.**

Sl. No.	In silico Properties	Curcumin	Metal Complexes
1	TPSA	93.06 Å	154.76 Å
2	H-Donors	2	4
3	H-acceptors	6	12
4	Rot-bonds	8	12
5	Drug Score	0.40	0.12

**Table 3: Physical and analytical information on Curcumin ligand and its metal complexes.**

Compound	Mol. Formula	Mol. Wt.(g/mol)	Colour	Physical state	MP°C
C	C <sub>21</sub> H <sub>20</sub> O <sub>6</sub>	368.38	Orange yellow	Solid	183
C1	C <sub>42</sub> H <sub>44</sub> CuO <sub>12</sub>	804.34	Dark green	Solid	352
C2	C <sub>42</sub> H <sub>44</sub> FeO <sub>12</sub>	796.64	Dark green	Solid	354
C3	C <sub>42</sub> H <sub>44</sub> CoO <sub>12</sub>	799.72	Dark green	Solid	345
C4	C <sub>42</sub> H <sub>44</sub> NiO <sub>12</sub>	799.48	Dark green	Solid	350
C5	C <sub>42</sub> H <sub>44</sub> ZnO <sub>12</sub>	806.17	Dark green	Solid	345
C6	C <sub>42</sub> H <sub>44</sub> HgO <sub>12</sub>	941.38	Dark green	Solid	352
C7	C <sub>42</sub> H <sub>44</sub> CdO <sub>12</sub>	853.20	Dark green	Solid	355
C8	C <sub>42</sub> H <sub>44</sub> SeO <sub>12</sub>	819.75	Dark green	Solid	354
C9	C <sub>42</sub> H <sub>44</sub> MgO <sub>12</sub>	766.10	Dark green	Solid	353
C10	C <sub>42</sub> H <sub>44</sub> CaO <sub>12</sub>	784.90	Dark green	Solid	350

shifted to a higher frequency region band at 1704 cm<sup>-1</sup>, indicating metal ion coordination.<sup>20</sup> Furthermore, in both circumstances, the aromatic or aliphatic -CH groups remain the same.<sup>21</sup> Finally, the FTIR spectra of Curcumin-metal complexes demonstrate the metal group's vibration absorption band M-O, in the frequency range 700-450 cm<sup>-1</sup>.

### **<sup>1</sup>H NMR spectrum**

The <sup>1</sup>H NMR spectra of Curcumin-metal complexes were obtained by using a solvent DMSO and Tetramethyl Silane (TMS)

as an internal standard at room temperature. Curcumin-metal NMR spectra compare the <sup>1</sup>H NMR spectrum of metal complexes to those of similar un-complexed compounds. Curcumin's interaction with metals was evidenced by changes in resonance signals. In the <sup>1</sup>H NMR spectra, the signal at 16.1 ppm linked to Curcumin's -OH proton disappeared in metal complexes. This disappearance signifies the deprotonation of the enolic group due to coordination with metals. Consequently, this confirms the attachment of oxygen to metal ions (C-O-M).<sup>22</sup> Protons from the ligand's phenolic -OH and -OCH<sup>3</sup> groups were detected at 9.68



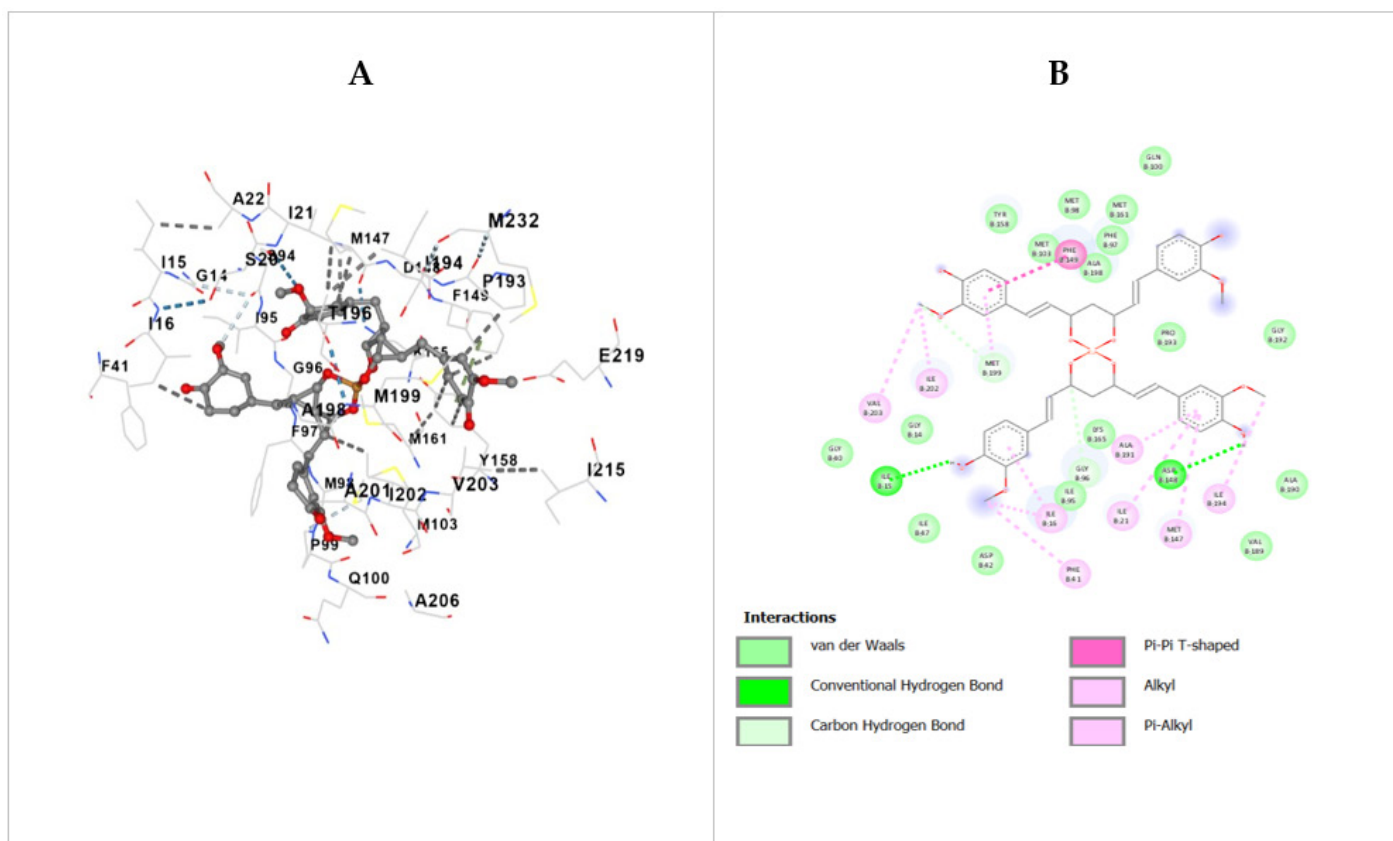


**Figure 2:** Interactions between C1 and 2NSD; (a) three-dimensional view and (b) two-dimensional view.

**Table 4:** Selectivity Index and  $IC_{50}$  of the synthesized compounds.

Sl. No.	Compound	MIC ( $\mu\text{g/mL}$ )	$IC_{50}$	Selectivity Index
1	C	20	7.7	0.4
2	C1	2.5	10.0	4.0
3	C2	2.5	9.6	3.8
4	C3	2.5	9.9	3.9
5	C4	5	9.1	1.8
6	C5	10	8.9	0.8
7	C6	10	9.3	0.9
8	C7	2.5	9.8	3.9
9	C8	5	8.7	1.7
10	C9	5	8.3	1.6
11	C10	10	8.9	0.9
12	Doxorubicin	5	7.3	1.5

ppm and 3.6 ppm, respectively. This findings suggests that these specific groups do not involved in the complexation process.<sup>23</sup>

### ESI mass spectral studies

The ligand's ESI mass spectrum revealed a dominant base peak at  $m/z=369$ , which corresponded to the expected mass  $[M+H]^+$  peak. The ESI mass spectrum of metal complexes displayed peaks at  $m/z=806$   $[M+H]^+$  for C1, 799  $[M+H]^+$  for C2, 780  $[M+H]^+$  for C3, 781  $[M+2H]^+$  for C4, 807  $[M+H]^+$  for C5, 943  $[M+H]^+$

for C6, 854  $[M+2H]^+$  for C7, 820  $[M+H]^+$  for C8, 768  $[M+2H]^+$  for C9, 785  $[M+H]^+$  for C10 complexes. In all metal complexes, the analytical results of molecular ions corresponded to the stoichiometry of metal to ligand molar ratio 1:2  $[M: L]$ .<sup>24</sup>

### X-ray diffraction analysis

X-ray diffraction studies of a synthesised metal Compound [C1] were performed from 0-100° Å. The P-XRD patterns of the Curcumin-Cu (II) [C1] complex, covering a range of 2 $\theta$  values

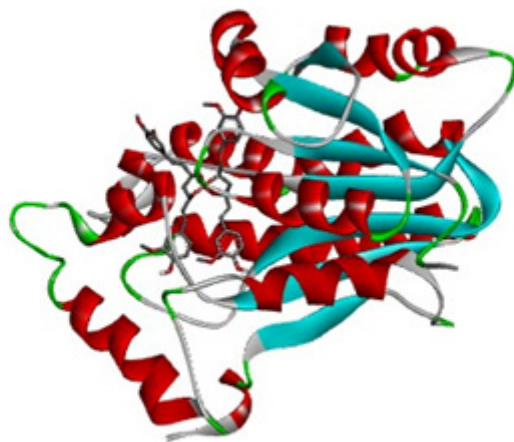


**Figure 3:** Docked view of C1 with 2NSD.

**Table 5:** IR Bands ( $\text{cm}^{-1}$ ) of Curcumin Ligand and its Metal Complexes.

Compound	OH ( $\text{cm}^{-1}$ )	C=O ( $\text{cm}^{-1}$ )	O-CH <sub>3</sub> ( $\text{cm}^{-1}$ )	Aliphatic C=C ( $\text{cm}^{-1}$ )	Aromatic C=C ( $\text{cm}^{-1}$ )	M-O ( $\text{cm}^{-1}$ )
C	3501	1626	2949	1500	1574	-
C1	3350	1707	2839	1506	1582	470
C2	3248	-	2932	1494	1589	645
C3	3345	1696	2932	1503	1592	520
C4	3325	1636	2933	1510	1598	560
C5	3294	-	2937	1491	1576	480
C6	3254	1701	2943	1498	1592	530
C7	3326	1696	2947	1503	1597	535
C8	3376	1656	2934	1492	1588	630
C9	3246	1628	2945	1508	1580	498
C10	3276	-	2936	1501	1587	576

from  $10^\circ$  to  $90^\circ$ .<sup>25</sup> The diffractogram provides information about the  $2\theta$  values corresponding to each peak, the relative intensity of the peaks and the interplanar spacing (d-values) between crystal lattice planes. These d-values were determined through equations such as Bragg's equation ( $n\lambda=2d\sin\theta$ ) or Scherrer's formula ( $d=0.89\lambda/\beta\cos\theta$ ), where 'd' signifies the average crystal size of the phase being analysed. In these equations, ' $\lambda$ ' represents the wavelength of the X-ray beam used ( $\lambda=1.5406 \text{ \AA}$ ), ' $\beta$ ' denotes the width of the diffraction peak at half its maximum intensity and ' $\theta$ ' corresponds to the Bragg's angle.<sup>26</sup> The metal complexes powder X-ray diffraction patterns were soluble in polar organic solvents, especially DMSO and DMF.<sup>27</sup> The diffractogram for sample C1 displays a total of 13 reflection peaks within the  $10^\circ$  to  $90^\circ$  range of  $2\theta$  angles. Notably, the maximum intensity peaks are found at  $16.27^\circ$ , corresponding to an interplanar spacing (d) of  $5.50 \text{ \AA}$ . The experimental and calculated interplanar spacing values are both provided in Table 5, along with their

corresponding relative intensities, particularly focusing on the most prominent peak. The presence of crystalline components in the complex may confirm by the extremely sharp peak.<sup>28</sup>

### Antitubercular activity and Cytotoxicity

The antitubercular activity was performed on the synthesized 10 Curcumin complexes C1 to C10 against *M. tuberculosis* (strain H37Rv) using the Isoniazid and Rifampicin as standards. On comparing the results obtained from the test we concluded C1 showed the highest activity and was the most sensitive at  $0.8 \mu\text{g/mL}$  when compared to all compounds and standard (Figure 4).

The *in vitro* cytotoxic studies was performed using Vero cells (ATCC CCL-81) for all synthesized compounds using doxorubicin as standard (Table 6). The metal complexes  $\text{IC}_{50}$  values were greater than the ligand's and the compound C1 showed highest MIC ( $2.5\text{g/mL}$ ), lesser toxicity with  $\text{IC}_{50}$  of 10.0

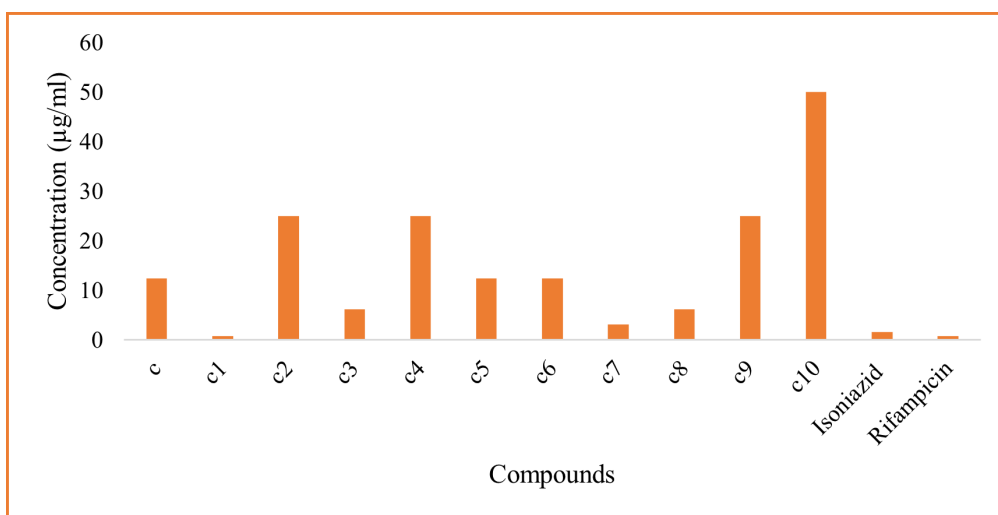


**Figure 4:** Graphical representation of Antitubercular activity of ligand and its metal complexes.

**Table 6:** Cu(II) complex[C1] powder X-ray data.

Peaks	2θ	θ	Sin θ	'd' in Å
1	16.27	8.13	0.14	5.50
2	22.06	11.03	0.19	4.08
3	23.86	11.93	0.20	3.85
4	26.69	13.34	0.23	3.34
5	28.54	14.27	0.24	3.20
6	34.08	17.04	0.29	2.65
7	38.12	19.06	0.32	2.40
8	40.85	20.42	0.34	2.26
9	43.13	21.56	0.36	2.13
10	47.47	23.73	0.40	1.92
11	49.31	24.65	0.41	1.87
12	56.36	28.18	0.47	1.63
13	57.39	28.69	0.48	1.60

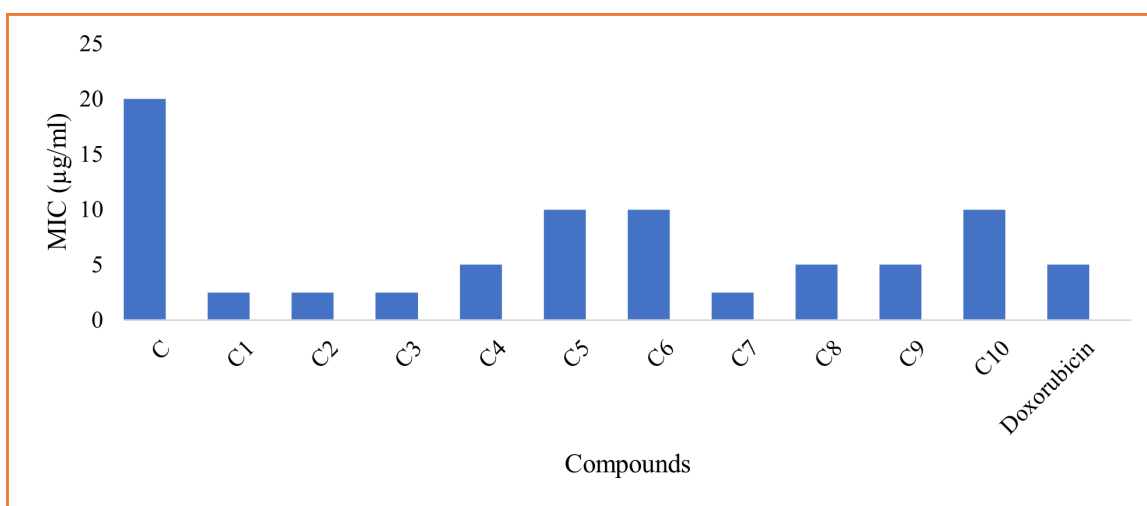


**Figure 5:** Graphical representation of Minimum Inhibitory Concentration.



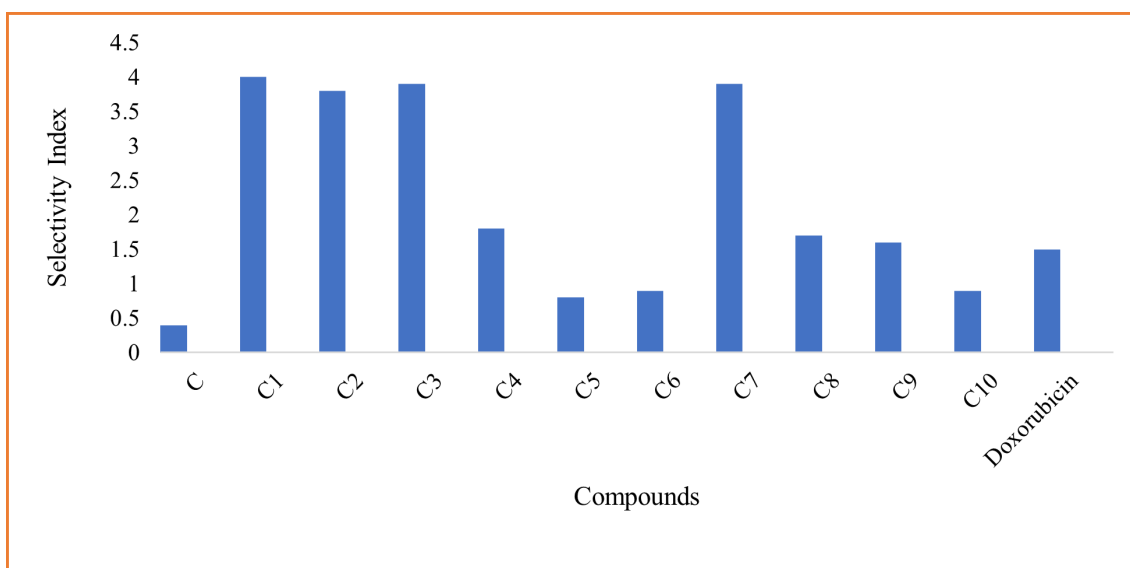


**Figure 6:** Graphical representation of Selectivity Index.

and selectivity index of 4.0 than compared to ligand molecule and other synthesized compounds (Figures 5 and 6).

## CONCLUSION

The main emphasis of this study revolves around the transition metal complexes that originate from Curcumin. The structural attributes of the synthesized compounds were elucidated through a range of analytical and spectroscopic methods, including FT-IR, <sup>1</sup>H NMR, mass spectrometry and Powder X-ray Diffraction (P-XRD) analysis. By employing MABA assay, metal complexes showed stronger antitubercular activity against *Mycobacterium tuberculosis* than ligand. The cytotoxic actions of the synthesised compounds were assessed using the MTT test and C1 was shown to have the highest MIC (2.5g/mL), IC<sub>50</sub> value (10.0) and selectivity index (4.0) among all other compounds. A molecular docking investigation was conducted on a set of ten compounds, assessing their binding affinities in conjunction with their pharmacological attributes and toxicity profiles. The results of this analysis pointed out that compound C1 exhibited the most elevated binding energy concerning the Enoyl CoA reductase. A good binding affinity of -10.1 'Kcal/mol' was identified, which is stabilised by two hydrogen bonds. As a result, among the proposed compounds, C1 (Curcumin-Cu complex) had the greatest activity with the highest IC<sub>50</sub> values.

## ACKNOWLEDGEMENT

We extend our sincere thanks to Krupanidhi College of Pharmacy for granting us access to their laboratory facilities. The authors are also grateful for the support from the Sophisticated Analytical Instrumentation Facility (SAIF) at Punjab University and spectrum data contributions from Vellore Institute of Technology. Special acknowledgment is reserved for Maratha Mandal's Central Research Laboratory for their provision of antitubercular activity

data, as well as the Division of Microbiology at CSIR-Central Drug Research Institute for conducting cytotoxicity tests.

## CONFLICT OF INTEREST

The authors declare that there are no conflict of interest.

## ABBREVIATIONS

%; Percentage; °C: Degree Celsius;  $\mu\text{mol}$ : Micro Mole; <sup>1</sup>H NMR: Proton Nuclear Magnetic Resonance; ATCC: American Type Culture Collection; DMSO: Dimethyl Sulphoxide; FTIR: Fourier Transform Infrared Spectroscopy; IC<sub>50</sub>: Half Maximal Inhibitory Concentration; M.P.: Melting Point; MABA: Microplate Alamar Blue Assay; MDR TB: Multidrug Resistant Tuberculosis; MIC: Minimum Inhibitory Concentration; Mmol: Milli Mole; ESI: Electron Spray Ionization; PDB: Protein Data Bank; TLC: Thin Layer Chromatography; TPSA: Topological Polar Surface Area; DCM: Dichloromethane; DMF: Dimethyl Formamide; CDCl<sub>3</sub>: Deuterated Chloroform; MHz: Megahertz; RPM: Revolutions Per Minute; PPM: Parts Per Million.

## SUMMARY

All 10 compounds of Curcumin metal complexes were docked against Enoyl acyl carrier protein reductase (ENR) and ADMET properties were evaluated. The Curcumin-Metal complexes were synthesized via, single step reaction known as complexation reaction, where it involved in the attachment of Metal salts. The progress of the reaction was monitored by TLC (Dichloromethane: Ethanol) (19:1) using gradient elution column chromatography. The synthesized compounds were characterized using FT-IR, <sup>1</sup>H NMR, MASS, P-XRD and solubility studies were performed. The compounds were evaluated to its activity using MABA assay. In these all compounds, C1 showed the best MIC ranging at 25  $\mu\text{g}/\text{ml}$  and 0.8  $\mu\text{g}/\text{ml}$ . The *in vitro* cytotoxicity

evaluation was performed to obtain % inhibition, IC<sub>50</sub> value and the selective index. It was done using MTT assay using tubercular cell lines representing *Mycobacterium tuberculosis* i.e., vero cells ATCC CCL-81.

## REFERENCES

- World Health Organization, Antimicrobial Resistance. <https://www.who.int/news-room/fact-sheets/detail/antimicrobial-resistance> (accessed on 19<sup>th</sup> Oct, 2021)
- Sinha A, Chaudhary R, Reddy DS, Kongot M, Kurjogi MM, Kumar A. ON donor tethered copper (II) and vanadium (V) complexes as efficacious anti-TB and anti-fungal agents with spectroscopic approached HSA interactions. *Heliyon*. 2022;8(8). <https://doi.org/10.1016/j.heliyon.2022.e10125>
- MacNeil A, Glaziou P, Sismanidis C, Maloney S, Floyd K. Global epidemiology of tuberculosis and progress toward achieving global targets-2017. *Morb Mortal Wkly Rep*. 2019;68(11):263. <https://doi.org/10.15585/mmwr.mm6811a3>
- Scarim CB, de Farias RL, de Godoy Netto AV, Chin CM, Dos Santos JL, Pavan FR. Recent advances in drug discovery against *Mycobacterium tuberculosis*: Metal-based complexes. *Eur J Med Chem*. 2021;214:113166. <https://doi.org/10.1016/j.ejmech.2021.113166>
- Affrose A, Parveen SD, Kumar BS, Pitchumani K. Selective sensing of silver ion using berberine, a naturally occurring plant alkaloid. *Sens Actuators B Chem*. 2015;206:170-5. <https://doi.org/10.1016/j.snb.2014.09.042>
- Maia PI, Pavan FR, Leite CQ, Lemos SS, de Sousa GF, Batista AA, et al. Vanadium complexes with thiosemicarbazones: Synthesis, characterization, crystal structures and anti-*Mycobacterium tuberculosis* activity. *Polyhedron*. 2009;28(2):398-406. <https://doi.org/10.1016/j.poly.2008.11.017>
- Pröhl M, Schubert US, Weigand W, Gottschaldt M. Metal complexes of curcumin and curcumin derivatives for molecular imaging and anticancer therapy. *Coord Chem Rev*. 2016;307:32-41. <https://doi.org/10.1016/j.ccr.2015.09.001>
- Mary CP, Vijayakumar S, Shankar R. Metal chelating ability and antioxidant properties of Curcumin-metal complexes-A DFT approach. *J Mol Graph Model*. 2018;79:1-4. <https://doi.org/10.1016/j.jmgm.2017.10.022>
- Syed HK, Iqbal MA, Haque RA, Peh KK. Synthesis, characterization and antibacterial activity of a curcumin-silver (I) complex. *J Coord Chem*. 2015;68(6):1088-100. <https://doi.org/10.1080/00958972.2014.1003051>
- Mahmoud WH, Omar MM, Sayed FN. Synthesis, spectral characterization, thermal, anticancer and antimicrobial studies of bidentate azo dye metal complexes. *J Therm Anal Calorim*. 2016;1071-89. <https://doi.org/10.1007/s10973-015-5172-1>
- Alahari A, Trivelli X, Guérardel Y, Dover LG, Besra GS, Sacchettini JC, Reynolds RC, Coxon GD, Kremer L. Thiacetazone, an antitubercular drug that inhibits cyclopropanation of cell wall mycolic acids in mycobacteria. *PLoS one*. 2007;2(12):e1343. <https://doi.org/10.1371/journal.pone.0001343>
- Mangwani N, Singh PK, Kumar V. Medicinal plants: adjunct treatment to tuberculosis chemotherapy to prevent hepatic damage. *J Ayurveda Integr Med*. 2020;11(4):522-8. <https://doi.org/10.1016/j.jaim.2019.02.004>
- Barua N, Buragohain AK. Therapeutic potential of curcumin as an antimycobacterial agent. *Biomolecules*. 2021;11(9):1278. <https://doi.org/10.3390/biom11091278>
- Morris GM, Goodsell DS, Halliday RS, Huey R, Hart WE, Belew RK, et al. Automated docking using a Lamarckian genetic algorithm and an empirical binding free energy function. *J Comput Chem*. 1998;19(14):1639-62. [https://doi.org/10.1002/\(SICI\)1096-987X\(19981115\)19:14<1639::AID-JCC10>3.0.CO;2-B](https://doi.org/10.1002/(SICI)1096-987X(19981115)19:14<1639::AID-JCC10>3.0.CO;2-B)
- Stryjska, I., Korona, G.L., Che, cin' ska. Synthesis, spectroscopy, single-crystal structure analysis and antibacterial activity of two novel complexes of Silver (I) with Miconazole drug. *Int J Mol Sci*. 2021;22(4). <https://doi.org/10.3390/ijms22041510>
- El-Ganiny AM, Gad AI, El-Sayed MA, Shaldam MA, Abbas HA. The promising anti-virulence activity of candesartan, domperidone and miconazole on *Staphylococcus aureus*. *Braz J Microbiol*. 2022;1-8. <https://doi.org/10.1007/s42770-021-00655-4>
- Guan L, Yang H, Cai Y, Sun L, Di P, Li W, et al. ADMET-score-a comprehensive scoring function for evaluation of chemical drug-likeness. *Med Chem Comm*. 2019;10(1):148-57. [10.1039/C8MD00472B](https://doi.org/10.1039/C8MD00472B)
- Petrou A, Fesatidou M, Geronikaki A. Thiazole ring-A biologically active scaffold. *Molecules*. 2021;26(11):3166. <https://doi.org/10.3390/molecules26113166>
- ZHENG X, Av-Gay Y. System for efficacy and cytotoxicity screening of inhibitors targeting intracellular *Mycobacterium tuberculosis*. *J Vis Exp*. 2017;(122):e55273. [10.3791/55273](https://doi.org/10.3791/55273)
- Shanthalakshmi K, Mahesh B, Belagali S. Synthesis of Benzothiazole Schiff's Bases and screening for the Antioxidant Activity. *J Chem Pharm. Res*. 2016;8(10):240-3. <https://doi.org/10.20959/wjpr20173-7808>
- Peni P, Sasri R, Silalahi IH. Synthesis of Metal-Curcumin Complex Compounds (M=Na<sup>+</sup>, Mg<sup>2+</sup>, Cu<sup>2+</sup>). *J kim Sains Apl*. 2020;23(3):75-82.
- Saritha TJ, Metilda P. Synthesis, spectroscopic characterization and biological applications of some novel Schiff base transition metal (II) complexes derived from curcumin moiety. *J Saudi Chem Soc*. 2021;25(6):101245. <https://doi.org/10.1016/j.jscc.2021.101245>
- Netalkar PP, Kamath A, Netalkar SP, Revankar VK. Design, synthesis and DNA binding activities of late first row transition metal (II) complexes of bi-functional tri- and tetra-topic imines. *Spectrochim. Acta A Mol Biomol Spectrosc*. 2012;97:762-70. <https://doi.org/10.1016/j.saa.2012.07.066>
- Rao NN, Gopichand K, Nagaraju R, Ganai AM, Rao PV. Design, synthesis, spectral characterization, DNA binding, photo cleavage and antibacterial studies of transition metal complexes of benzothiazole Schiff base. *Chem Data Collect*. 2020;27:100368. <https://doi.org/10.1016/j.cdc.2020.100368>
- Dhanaraj CJ, Nair MS. Synthesis and characterization of metal (II) complexes of poly (3-nitrobenzylidene-1-naphthylamine-co-succinic anhydride). *Eur Polym J*. 2009;45(2):565-72. <https://doi.org/10.1016/j.eurpolymj.2008.11.011>
- Gavhane VS, Rajbhoj AS, Gaikwad ST. X-ray diffraction study and biological analysis of transition metal complexes of N-4-disubstituted thiosemicarbazone. *Res J Chem Sci*. 2015;33-37.
- Kirthan BR, Prabhakara MC, Naik HB, Nayak PA, Naik EI. Synthesis, characterization, DNA interaction and anti-bacterial studies of Cu (ii), Co (ii) and Ni (ii) metal complexes containing azo-dye ligand. *Chem Data Collect*. 2020;29:100506. <https://doi.org/10.1016/j.cdc.2020.100506>
- Sarkar S, Nag SK, Chattopadhyay AP, Dey K, Islam SM, Sarkar A, Sarkar S. Synthesis, structure and catalytic activities of nickel (II) complexes bearing N4 tetradentate Schiff base ligand. *J Mol Struct*. 2018; 1160:9-19. <https://doi.org/10.1016/j.molstruc.2018.01.035>

**Cite this article:** Yamuna HM, Das P, Harshashree M, Dang R. Metal Complexes of Curcumin: A Comprehensive Approach to Design, Synthesis, Characterization and Assessment of Antitubercular Activity. *Indian J of Pharmaceutical Education and Research*. 2024;58(3s):s963-s972.